JOURNAL OF AGRICULTURAL AND FOOD CHEMISTRY

Article

pubs.acs.org/JAFC

Detection of Aflatoxin M1 in Milk by Dynamic Light Scattering Coupled with Superparamagnetic Beads and Gold Nanoprobes

Zhong Zhang, Mengshi Lin,* Sha Zhang, and Bongkosh Vardhanabhuti

Food Science Program, Division of Food Systems & Bioengineering, University of Missouri, Columbia, Missouri, United States 65211-5160

ABSTRACT: This study aimed to develop a rapid and sensitive method for detection of aflatoxin M1 (AFM) by dynamic light scattering (DLS) coupled with superparamagnetic beads and gold nanoprobes. The nanoprobes were synthesized by the conjugate of AFM and bovine serum albumin (AFM-BSA), BSA, and gold nanoparticles. Magnetic beads-based immunosorbent assay (MBISA) was used to measure the concentration of AFM by direct competition between AFM and nanoprobes. DLS was used to determine the concentration of unattached nanoprobes that was positively proportional to the concentration of AFM in the sample. TEM images prove that the as-prepared nanoprobes were able to attach on the magnetic beads through the antibody−antigen reaction. Compared to conventional ELISA, MBISA could effectively reduce the incubation time to 15 min in buffer solution and completely eliminate the color development step, thus simplifying the analysis of AFM. A linear relationship was observed between the inhibition values and the concentrations of AFM in both buffer solution (0−1000 ng·L^{-1}) and spiked milk samples (0−400 ng·L^{-1}). The limit of detection was found to be 37.7 ng·L^{-1} for AFM in buffer solution and 27.5 ng·L^{-1} in milk samples. These results demonstrate that DLS coupled with magnetic beads and gold nanoprobes is a rapid and effective method to detect AFM. This method could also be easily extended to rapid detection of other mycotoxins and biological species.

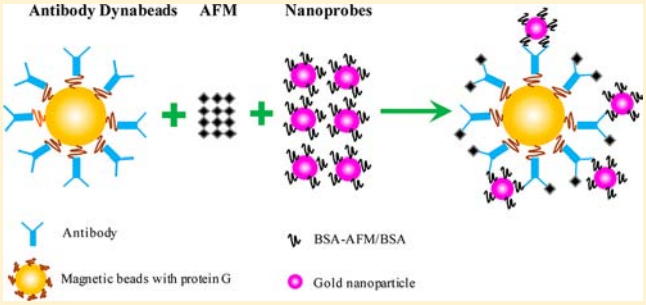

KEYWORDS: *DLS, gold nanoprobes, magnetic beads, aflatoxin M1, MBISA*

INTRODUCTION

Aflatoxin M1 (AFM), a hydroxylated metabolite of aflatoxin B_1, is often found in milk from animals fed with aflatoxin B1-contaminated feeds.[1,2] AFM can also be found in a variety of dairy products such as cheese, yogurt, and infant formula due to its resistance to heat treatment. [3] AFM is a carcinogenic, genotoxic, and immunosuppressive compound. Therefore, the contamination of foods by AFM could pose a serious risk to public health, especially to milk consumers.[4−6] In 1977, the U.S. Food and Drug Administration (FDA) established a strict action level of 500 ng·L^{-1} for AFM in fluid milk.[7]

Currently, several qualitative and quantitative methods have been developed to detect AFM in milk and other dairy products.[8−10] Among them, thin layer chromatography and immunochromatographic assay are the most commonly used methods for rapid qualitative detection and semiquantification of aflatoxins.[8,10,11] In addition, some biosensors have also been developed to analyze the AFM, including electrochemical immunochip sensor and DNA-based electrochemical membrane.[12−14] The quantification of AFM is usually conducted by high performance liquid chromatography (HPLC) and enzyme-linked immunosorbent assay (ELISA).[9,15,16] The HPLC fluorimetric detection method can quantify AFM with high accuracy and a very low detection limit, but it requires complex and laborious pretreatments of samples, such as defatting of milk and subsequent extraction of AFM by methanol or immunoaffinity columns.[17] The ELISA methods employ a direct competition of AFM and AFM-HRP (horseradish peroxidase) for binding sites of the antibody that are coated on microtiter wells. Compared to HPLC methods, ELISA requires fewer sample pretreatment procedures and has higher throughput.[18] It is now commonly used in the AFM analysis. However, the ELISA still requires 30−60 min incubation time for the equilibrium of antibody−antigen reaction, 15 min for the development of color, and around 10 min for spectrophotometric assay.[19]

Dynamic light scattering (DLS) is a technique that can be used to measure the concentration and hydrodynamic diameter of micro- and nanoparticles dispersed in water solution. The detection limit could be as low as 5.95×10^{-13} M using 40 nm gold nanoparticles.[20] Due to its high sensitivity, simple operation, and rapid data acquisition, DLS technique coupled with gold nanoprobes is becoming one of the most widely used methods for detection of chemical and biological species.[21] For example, DLS has been used to diagnose prostate cancer by correlating the average size of nanoprobes with the concentration of prostate specific antigen.[22] But it is difficult

Received: February 19, 2013
Revised: April 19, 2013
Accepted: April 19, 2013
Published: May 2, 2013

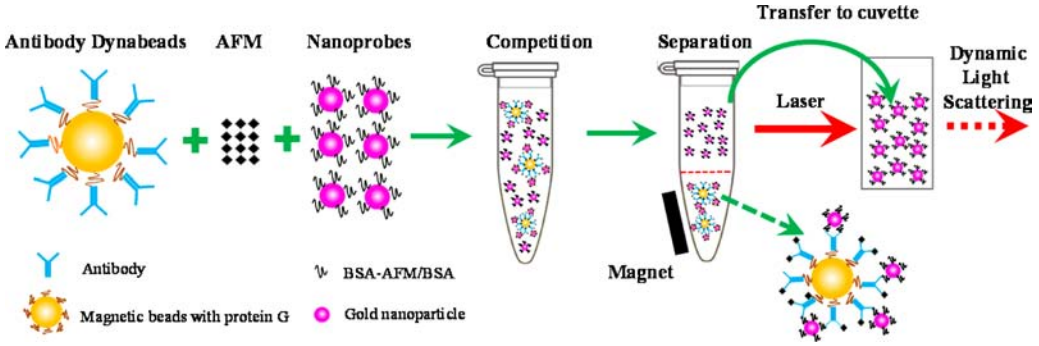

Figure 1. Detection of AFM by dynamic light scattering (DLS) using magnetic beads separation and gold nanoprobes.

to directly apply this method for qualification of AFM because AFM could not be sandwiched by antibody-modified nanoprobes. However, the correlation of DLS intensity with the concentration of gold nanoparticles opens a new route for us to detect AFM using gold nanoprobes modified with competing antigen.

Herein, we aim to develop a rapid detection method for AFM by DLS coupled with gold nanoprobes and magnetic beads. Gold nanoparticles were labeled with the conjugate of AFM and bovine serum albumin (AFM-BSA). The AFM-BSA can be anchored on the surface of gold nanoparticles through the abundant surface lysine groups of AFM-BSA.[23] In addition, the anti-AFM antibody could be easily linked on the surface of magnetic beads by the oriented coupling effect of recombinant protein G.[24] Unlike the immobilized antibody of conventional ELISA, these antibody-modified magnetic beads act as small "hunters" and can rapidly capture AFM when they are dispersed in the sample solution containing AFM, therefore reducing the incubation time. As illustrated in Figure 1, the AFM competes with gold nanoprobes for the binding sites of antibody on magnetic beads. After incubation, the bulk solution was separated from the magnetic beads by a magnet and directly transferred into a cuvette for DLS analysis. The DLS intensity of nanoprobe in bulk solution is positively proportional to the concentration of AFM in sample solution.

MATERIALS AND METHODS

Materials and Chemicals. An immunoprecipitation kit and a magnet were obtained from Invitrogen (Carlsbad, CA, U.S.). This kit contained 2 mL of magnetic beads protein G, 16 mL of antibody binding and washing buffer, 28 mL washing buffer and 1 mL of elution buffer. A rabbit polyclonal antibody to AFM (100 μL) was purchased from Antibody-online (Atlanta, GA, U.S.). Bovine serum albumin (BSA), AFM, AFM-BSA conjugate (4−8 mol AFM per mol BSA), disodium hydrogen phosphate, sodium dihydrogen phosphate, sodium citrate, and gold chloride (30 wt % in HCl) were purchased from Sigma-Aldrich (St. Louis, MO, U.S.) and used without further purification. Tween 20, 4-mercaptopyridine, and cuvettes were obtained from Fisher Scientific (Rochester, NY, U.S.).

Fabrication of Gold Nanoparticles and Gold Nanoprobes. Gold nanoparticles with an average diameter of 32 nm were fabricated by the citrate reduction method.[25] Specifically, 250 mL ultrapure water was stirred and heated to boiling temperature on a magnet stirrer/hot plate. $HAuCl_4$ (40 μL) was then added to the boiling water. Subsequently, 2.7 mL sodium citrate solution (1 wt %) was injected into the flask to reduce $HAuCl_4$ to gold nanoparticles. The mixture was boiled for 5 min and then cooled to room temperature. The as-prepared gold nanoparticles (0.5 mL) and AFM-BSA (5 nM, 0.5 mL) solution were thoroughly mixed in a 1.5 mL centrifuge tube (Eppendorf, Hamburg, Germany). After 40 min, 100 μL of 1% BSA solution was added to prevent the aggregation of nanoparticles and block the bare surface of nanoparticles. Then, 200 μL of 4-mercaptopyridine (10 μM) were added to the mixture to further block the surface of gold nanoparticles. After 20 min incubation at room temperature, the excess 4-mercaptopyridine, BSA, and AFM-BSA conjugate were removed by centrifugation for 4 min at 8400 rpm (Eppendorf MiniSpin, Hamburg, Germany). Following the removal of the supernatant, the red oily precipitate was dispersed in 0.5 mL of phosphate buffer solution (PBS, pH 7.4, 10 mM) and subjected to a second centrifugation. The nanoprobes were finally dispersed in 0.5 mL PBS and stored at 4 °C.

Preparation of Antibody-Magnetic Beads Complex. A volume of 15.0 μL of magnetic beads was transferred to a 1.5 mL centrifuge tube. The magnetic beads were washed three times by the antibody binding and washing buffer. The magnetic beads were then suspended in 0.5 mL of antibody solution (Dilution 1:3000). The magnetic beads were incubated for 60 min with 300 rpm rotation at room temperature. After incubation, the magnetic beads were washed three times by washing buffer and finally suspended in 1.5 mL of washing buffer. The fragment crystallizable region (Fc region) of antibody was successfully attached on the magnetic beads by the coupling of recombinant protein G. The antibody-magnetic beads complex was prepared freshly to avoid the loss of activity during storage.

Analysis of AFM in PBS and Milk. An aliquot of antibody magnetic beads (100 μL) was transferred to a 1.5 mL tube. The magnetic beads were separated from the bulk solution by a magnet. After removing the liquid, 100 μL of AFM standard solution (0−2000 $ng \cdot L^{-1}$) and 60 μL of nanoprobe solution were added to the tube. The mixtures were incubated at room temperature for 15 min with a rotation speed of 300 rpm to allow for full competition of AFM and AFM-BSA modified nanoprobes. The magnetic beads were then absorbed tightly at the bottom of tube caused by magnetic attraction force from the magnet. The bulk solution (100 μL) was directly transferred into a cuvette prefilled with 1.2 mL high purity water for DLS analysis.

Skim milk was purchased from a local grocery store and spiked with AFM standard solution (v/v: 9:1). The analysis of skim milk was slightly different from that in PBS to avoid potential interaction between gold nanoprobes and milk proteins. First, 100 μL solution of antibody modified magnetic beads was added into spiked milk (100 μL) and incubated for 15 min at room temperature to capture AFM. The magnetic beads were then washed four times by antibody washing buffer (PBS, pH 7.4, 10 mM). Nanoprobe solution (60 μL) and PBS (100 μL) were subsequently added in the tube and incubated at room temperature for 25 min with rotation. After separation from magnetic beads, the bulk solution was subjected to DLS analysis as described above.

DLS measurements were performed at 25.0 ± 0.1 °C using a Malvern ZS ZEN 3600 system (Malvern, Worcestershire, U.K.) equipped with a red laser (633 nm). During the measurement, light from laser was directed and focused on the cuvette with 1.2 mL sample solution. The DLS signals were collected by a photodiode detector (Malvern, Worcestershire, U.K.) and processed by Malvern Zetasizer

dx.doi.org/10.1021/jf400043z | J. Agric. Food Chem. 2013, 61, 4520−4525

nanoapplication software. For each sample, two DLS measurements were conducted with at least 12 runs and each run lasted 10 s.

Transmission Electron Microscopy (TEM) Analysis. TEM (JEOL 1400, Tokyo, Japan) was used to visualize the reaction between gold nanoprobes and antibody on magnetic beads. After being incubated as described in the section 2.4, the magnetic beads were washed three times by PBS (pH = 7.4, 10 mM) and redispersed in 100 μL of PBS. A drop of magnetic beads solution (2 μL) was deposited on carbon side of copper/carbon grid and the grid was dried at room temperature for characterization by TEM.

Data Analysis. The OriginPro software (version 8.0, OriginLab, MA, USA) was used to analyze the data. The inhibition value was calculated by the following equation:

$$\%\text{inhibition} = \frac{I - I_0}{I_{Sat} - I_0} \times 100$$

where I is the DLS intensity obtained from different concentration of AFM, I_{Sat}, and I_0 are the DLS intensities corresponding to the saturating and noncompetitor antigen, respectively. The limit of detection (LOD) was calculated as the concentration corresponding to 10% of inhibition value.[24]

RESULTS AND DISCUSSIONS

Synthesis of Gold Nanoprobes. Figure 2 shows a TEM image of gold nanoparticles and the hydrodynamic diameter distribution of pure gold nanoparticles and AFM-BSA modified gold nanoparticles. The as-prepared gold nanoparticles were monodispersed with an average diameter of 32.0 ± 3.6 nm, as tested by TEM (Figure 2a). The size of the gold nanoparticles

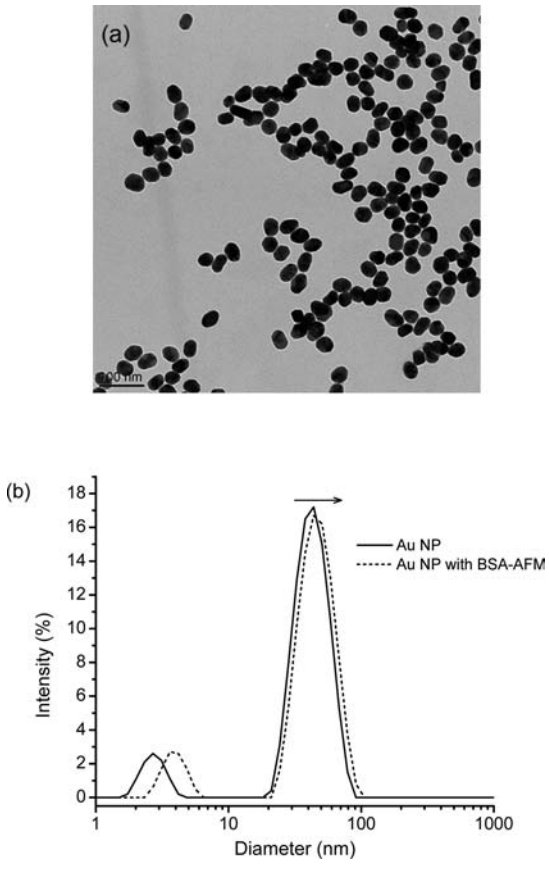

Figure 2. Characterization of gold nanoparticles and gold nanoprobes: (a) TEM image of gold nanoparticles (32.0 ± 3.6 nm); (b) size distribution of gold nanoparticles without and with AFM-BSA as determined by DLS.

plays an important role in developing a detection method by DLS because larger nanoparticles scatter light much stronger than smaller ones.[20] From Rayleigh approximation, the DLS intensity of 32 nm gold nanoparticles is 1072 times higher than that of 10 nm nanoparticles. Thus, it is important to use larger nanoparticles to enhance the sensitivity and lower the detection limit. Herein, 32 nm gold nanoparticles were chosen to fabricate the nanoprobes because they could easily be synthesized by the citrate reduction method with high reproducibility. Seed-mediated growth method is usually needed to produce gold nanoparticles with size of larger than 40 nm. The aspect ratio of gold nanoparticles used in this study was from 1.04 to 1.22, showing a spherical shape of nanoparticles. The AFM-BSA could bind uniformly on the surface of spherical gold nanoparticles. It is also important to keep a narrow size distribution for the gold nanoparticles to reduce the variation of DLS intensities.

The hydrodynamic diameter of gold nanoparticles increased around 5 nm when AFM-BSA was added, indicating successful attachment of AFM-BSA onto the surface of gold nanoparticles (Figure 2b). There are abundant functional groups that enable the adsorption of AFM-BSA and BSA onto the surface of gold nanoparticles, for example, amine groups from 60 surface lysines, imidazole group from histidine, and thiol group from cysteine. Therefore, BSA and AFM-BSA could spontaneously bind onto gold nanoparticles by direct coupling of those functional groups with gold through electrostatic interactions and coordination effects.[26] In addition, the hydrophobic interaction of BSA with gold also facilitated the immobilization of BSA on gold nanoparticles. It is worth noting that a small peak was also observed from 1.5 to 6 nm for both gold nanoparticles and gold nanoprobes in DLS size distribution, which contributed around 10% for total DLS intensity. Similar peaks (<10 nm) were also reported for 60 nm gold nanoparticle which was tested by the same type of Zetasizer. A previous study proved that the small peak was caused by the rotational motion of the nanoparticles because the gold nanoparticles were not perfectly spherical.[27] Likewise, a small peak observed in Figure 2b may be due to the rotational motion of the nanoparticles that were not perfectly spherical.

In this reaction, AFM-BSA acted as the competing antigen for AFM, and BSA was used as a stabilizing agent for the nanoprobes. BSA could also block the interaction between gold nanoparticles and antibodies on magnetic beads, thus reducing the nonspecific adsorption of nanoprobes on magnetic beads. Due to the large size of BSA molecules, the surface of gold nanoparticles may not be fully blocked by the addition of BSA. A small molecule with a thiol group, 4-mercaptopyridine, was added to fill the gaps between BSA molecules. During the double centrifugation, 4-mercaptopyridine also enhanced the stability of gold nanoprobes and prevented the aggregation of gold nanoprobes. Without using 4-mercaptopyridine, gold nanoprobes aggregated upon the first centrifugation even when 500 μL of BSA (5%) was present and could not be redispersed in solution. The possible explanation is that the AFM-BSA/BSA-coated gold nanoparticle contacted closely with each other during the centrifugation. The BSA molecule penetrated the adjacent gold nanoparticle surface, resulting in the coagulation of nanoprobes. On the contrary, this coagulation could be effectively prevented due to steric hindrance if 4-mercaptopyridine was covalently adsorbed on gold nanoparticles.

Preparation of Antibody-Magnetic Beads Complex. Protein G, a surface protein expressed by *Streptococcus*, has been widely used for binding the Fc region of immunoglobulin G (IgG).[28] The protein G has great affinity to polyclonal IgG of rabbit, goat, rat, and mouse. In the present study, a recombinant protein G was used to immobilize the anti-AFM antibody on the surface of magnetic beads. The nanoprobes would not bind with recombinant protein G due to repulsion between the hydrophilic surface of protein G and the hydrophobic surface of BSA. The optimum pH is 5.0 for the coupling reaction of antibody and protein G, while the antibody−antigen reaction is favored at pH 7.0. Therefore, it is necessary to adjust the pH by washing the magnetic beads with PBS of pH 7.4.

Correlation of DLS Intensity with the Concentration of Nanoprobes. Figure 3 shows a linear relationship between

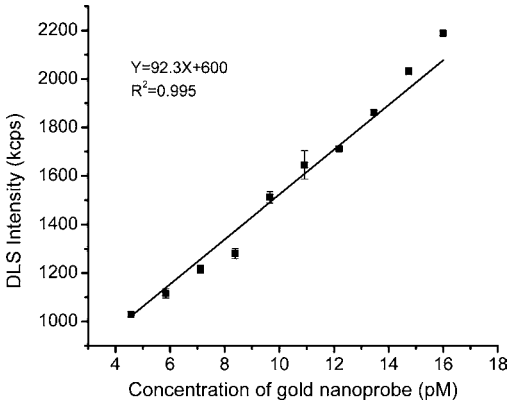

Figure 3. The linear relationship between the DLS intensity and the concentration of gold nanoprobes.

DLS intensity and the concentrations of gold nanoprobes (R^2 value = 0.995). In this situation, the total intensities were used, although there is a small peak from 1.5−6 nm (~10% of total intensity) that is also from nanoprobes as mentioned above. The standard deviations of DLS intensities were very small for the tested concentrations. These results indicate that the DLS intensity could be used to precisely predict the concentration of nanoprobes. With the protection of AFM-BSA/BSA, the nanoprobes were less liable to aggregate when dispersed in water solution, thus enabling the accurate detection of AFM by DLS.

Optimization of the Incubation Time. Figure 4 shows the changes in the DLS intensity during different incubation times when the nanoprobes were incubated with antibody modified magnetic beads in PBS. It was observed that the DLS intensity decreased with increased incubation time. The results indicate that gold nanoprobes were gradually adsorbed on the magnetic beads, resulting in lower concentration of nanoprobes in bulk solution. The DLS intensity decreased rapidly in the first 15 min while changed slowly between 15 and 25 min. The final equilibrium of the antibody−antigen reaction might not be reached within 15 min. But in this study, 15 min was selected as the optimum incubation time because a small difference was observed for the DLS intensity from 15 to 25 min. In conventional ELISA, the specific antibody is restrained on a small area of microtiter wells and stayed static in the sample solution. The antibody waits for antigen to be captured in the reaction.[19] On the contrary, in this experimental design, the antibody on the magnetic beads could move along with the movement of the antibody-magnetic beads complex. There

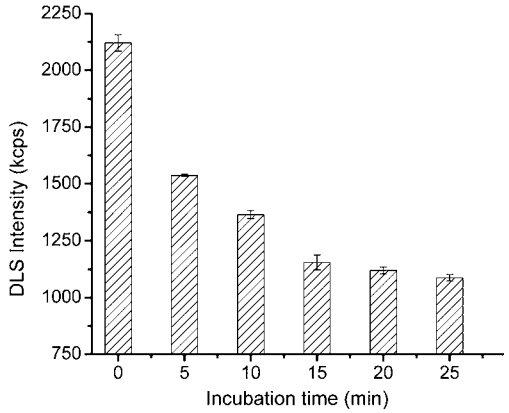

Figure 4. Optimization of incubation time for gold nanoprobes (60 μL) incubated with antibody modified magnetic beads in PBS (100 μL).

were tremendous amounts of microsized magnetic beads dispersed in the solution to hunt for AFM and nanoprobes. Meanwhile, the large surface area of the magnetic beads also facilitated the interaction of the antibody/antigen at room temperature. The incubation time was thus reduced for the aforementioned reasons. The optimized incubation time was 15 min, based on the antibody concentration used in this study.

Measurement of AFM in PBS by DLS. MBISA is based on direct competition between the nanoprobes and AFM for the antibody binding sites on magnetic beads (Figure 1). The antibody has stronger affinity to AFM than AFM-BSA modified gold nanoprobes. The concentration of nanoprobes attached on the surface of magnetic beads is negatively proportional to the concentration of AFM. Hence, the concentration of nanoprobes in bulk solution is positively proportional to the concentration of AFM in the sample solution. After competition with AFM, the nanoprobes in bulk solution could be separated from magnetic beads by a magnet and then measured by DLS. More importantly, the color development step and spectrophotometric analysis in conventional ELISA was substituted by direct DLS analysis of nanoprobes. The DLS measurement could be finished within a short time for each sample, thus significantly simplifying the analysis. Figure 5 shows the TEM images that were used to visualize and confirm the linkage of nanoprobes and antibodies on the magnetic beads. It was clearly shown that gold nanoprobes were adsorbed on the surface of magnetic beads due to the antibody−antigen reaction, which proved that AFM-BSA modified gold nanoparticles triggered the antibody−antigen reaction and could be used as a probe for AFM.

Figure 6 shows a linear relationship between the inhibition values and the concentrations of AFM in PBS (R^2 = 0.912). AFM has the preference to bind on the antibody binding site due to higher affinity and lower steric hindrance compared to AFM-BSA immobilized on gold nanoparticles. The antibody binding sites were first occupied by AFM. Thus, the number of remaining binding sites for nanoprobes was reduced when the concentration of AFM increased, resulting in a higher concentration of nanoprobes in the bulk solution. We also observed that there was no obvious change of DLS intensity when the concentration of AFM is higher than 1000 ng·L^{-1}. Thus, the saturation point of AFM is at 1000 ng·L^{-1} in PBS. Therefore, a linear relationship were only acquired for AFM between 0 and 1000 ng·L^{-1}. It is worth noting that the standard

dx.doi.org/10.1021/jf400043z | J. Agric. Food Chem. 2013, 61, 4520−4525

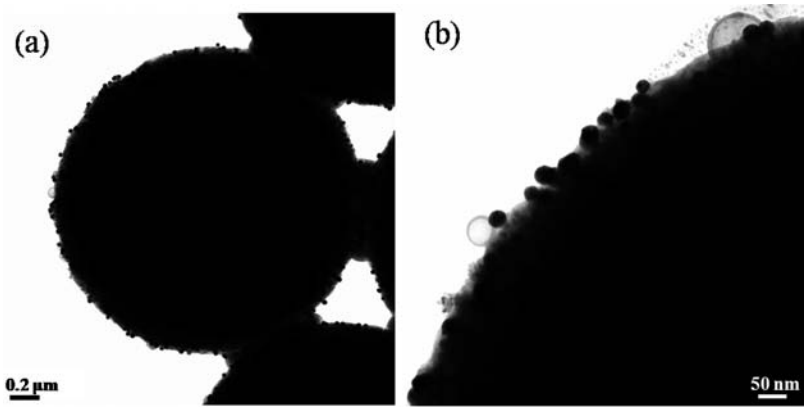

Figure 5. TEM images of nanoprobes attached on the magnetic beads with different magnifications: (a) scale bar: 0.2 μm; (b) scale bar: 50 nm.

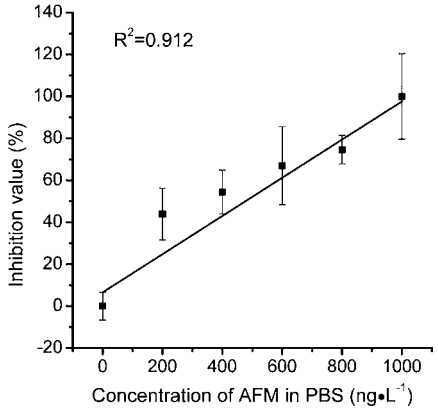

Figure 6. The linear relationship between the inhibition value and the concentration of AFM in PBS (0−1000 ng·L^{-1}).

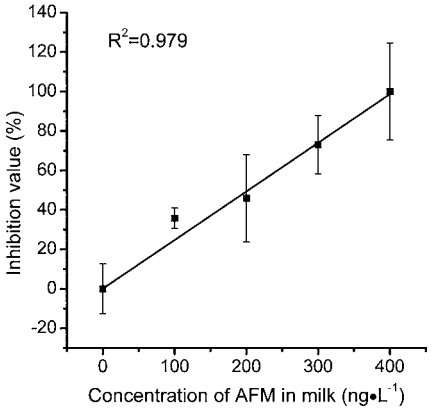

Figure 7. The linear relationship between the inhibition value and the concentration of AFM in skim milk (0−400 ng·L^{-1}).

deviation of the inhibition values is relatively high, which may be due to the fact that the polyclonal antibody serum may contain a heterogeneous complex mixture of antibodies with different affinity to AFM. Additionally, it is difficult to fabricate gold nanoparticles with uniform sizes. Although the standard deviation of gold nanoparticle size (32.0 nm) was only 3.6 nm, it still contributed to a relative standard deviation of 11.3%. The variation in size of gold nanoparticles could impact the DLS intensity directly, which also contributed to the high standard deviation of the inhibition values. The LOD in PBS was around 37.7 ng·L^{-1}, as estimated by 10% of the inhibition value.

Measurement of AFM in Milk by DLS. Although a layer of BSA was formed on the surface of the gold nanoprobes, proteins in milk might still be able to interact with gold nanoparticles, which may influence the reaction between antibodies and nanoprobes, resulting in a great interference for analysis. Therefore, the protocol for analysis of AFM in milk was modified to avoid this direct interaction between milk proteins and the nanoprobes. The magnetic beads were used to capture free AFM in milk and were thoroughly washed before incubation with gold nanoprobes.

Figure 7 shows a linear relationship between the inhibition value and the concentration of spiked AFM in skim milk. The linear range is much narrower than that in PBS. There were two reasons for this much lower saturation point (400 ng·L^{-1}) in milk compared to that in PBS (1000 ng·L^{-1}). First, the proteins or other components in milk, such as bovine IgG and mycotoxins, may occupy some of the antibody binding sites on the magnetic beads, rendering a higher concentration of nanoprobes in the bulk solution and a lower saturation point. Second, the protein G on magnetic beads might also adsorb some milk proteins, burying some antibody binding sites and enhancing steric hindrance for nanoprobes. Therefore, a linear relationship was only observed between the inhibition value and the concentration of AFM (R^2 = 0.979) when the concentration was between 0 and 400 ng·L^{-1} instead of 0−1000 ng·L^{-1}. The LOD of AFM in milk was around 27.5 ng·L^{-1}, as estimated by 10% of the inhibition value. The disadvantage of this method for detecting AFM in milk is that the AFM has to be extracted by antibody-magnetic beads before competing with gold nanoprobes. The detection time was also increased due to matrix effects of the milk. Nonetheless, the method is simple, specific, and opens a new route for detection of other mycotoxins in animal feeds and food samples.

In summary, the nanoprobes for AFM detection were successfully synthesized by AFM-BSA, BSA, 4-mercaptopyridine, and gold nanoparticles. MBISA coupled with DLS was used to determine the concentration of AFM by competition between AFM and gold nanoprobes. Compared to conventional ELISA, MBISA does not require the color development step, thus simplifying the analysis of AFM. The incubation time was 15 min in this study. Moreover, TEM images prove that nanoprobes were successfully attached on the magnetic beads via reaction between antibodies and nanoprobes. The concentration of AFM in solution was positively proportional to the concentration of nanoprobes as determined by DLS. A linear relationship was observed between the inhibition values

and the concentration of AFM for both PBS and spiked milk samples. The LOD was 37.7 ng·L^{-1} for AFM in PBS and 27.5 ng·L^{-1} in skim milk. This method could also be easily extended to rapid detection of other mycotoxins and biological species.

AUTHOR INFORMATION

Corresponding Author

*Tel: (573) 884-6718; fax (573) 884-7964; e-mail: linme@missouri.edu.

Notes

The authors declare no competing financial interest.

ACKNOWLEDGMENTS

The authors thank the Electron Microscopy Center (EMC) at the University of Missouri for its assistance in the TEM characterization. This research was supported by the USDA NIFA Nanotechnology Program Project No. 2011-67021-30391 and the University of Missouri Research Board.

REFERENCES

(1) Galvano, F.; Galofaro, V.; Galvano, G. Occurrence and Stability of Aflatoxin M1 in Milk and Milk Products: A Worldwide Review. *J. Food Protect.* **1996**, *59*, 1079−1090.

(2) Prandini, A.; Tansini, G.; Sigolo, S.; Filippi, L.; Laporta, M.; Piva, G. on the Occurrence of Aflatoxin M1 in Milk and Dairy Products. *Food Chem. Toxicol.* **2009**, *47*, 984−991.

(3) Stoloff, L.; Trucksess, M.; Hardin, N.; Francis, O. J.; Hayes, J.; Polan, C.; Campbell, T. Stability of Aflatoxin M in Milk. *J. Dairy Sci.* **1975**, *58*, 1789−1793.

(4) Reddy, K.; Salleh, B.; Saad, B.; Abbas, H.; Abel, C.; Shier, W. an Overview of Mycotoxin Contamination in Foods and Its Implications for Human Health. *Toxin Rev.* **2010**, *29*, 3−26.

(5) Chu, F. S. Mycotoxins: Food Contamination, Mechanism, Carcinogenic Potential and Preventive Measures. *Mutat. Res-Gen.Tox. En.* **1991**, *259*, 291−306.

(6) Eaton, D. L.; Gallagher, E. P. Mechanisms of Aflatoxin Carcinogenesis. *Annu. Rev. Pharmacol.* **1994**, *34*, 135−172.

(7) Wood, G. E.; Trucksess, M. W. Regulatory Control Programs for Mycotoxin-Contaminated Food. In *Mycotoxins in Agriculture and Food Safety*; CRC Press: Boca Raton, FL, 1998; pp 459−481.

(8) Iha, M. H.; Barbosa, C. B.; Favaro, R. M. D.; Trucksess, M. W. Chromatographic Method for the Determination of Aflatoxin M1 in Cheese, Yogurt, and Dairy Beverages. *J. AOAC Int.* **2011**, *94*, 1513−1518.

(9) Rodriguez Velasco, M. L.; Calonge Delso, M. M.; Ordonez Escudero, D. ELISA and HPLC Determination of the Occurrence of Aflatoxin M(1) in Raw Cow'S Milk. *Food. Addit. Contam.* **2003**, *20*, 276−80.

(10) Wang, J.-J.; Liu, B.-H.; Hsu, Y.-T.; Yu, F.-Y. Sensitive Competitive Direct Enzyme-Linked Immunosorbent Assay and Gold Nanoparticle Immunochromatographic Strip for Detecting Aflatoxin M1 in Milk. *Food Control* **2011**, *22*, 964−969.

(11) Xiulan, S.; Xiaolian, Z.; Jian, T.; Xiaohong, G.; Jun, Z.; Chu, F. S. Development of an Immunochromatographic Assay for Detection of Aflatoxin B1 in Foods. *Food Control* **2006**, *17*, 256−262.

(12) Banitaba, M. H.; Davarani, S. S.; Mehdinia, A. Study of Interactions between DNA and Aflatoxin B1 Using Electrochemical and Fluorescence Methods. *Anal. Biochem.* **2011**, *411*, 218−22.

(13) Siontorou, C. G.; Nikolelis, D. P.; Miernik, A.; Krull, U. J. Rapid Methods for Detection of Aflatoxin M1 Based on Electrochemical Transduction by Self-Assembled Metal-Supported Bilayer Lipid Membranes (s-BLMs) and on Interferences with Transduction of DNA Hybridization. *Electrochim. Acta* **1998**, *43*, 3611−3617.

(14) Tombelli, S.; Mascini, M.; Scherm, B.; Battacone, G.; Migheli, Q. DNA Biosensors for the Detection of Aflatoxin Producing *Aspergillus flavus* and *A. parasiticus*. *Monatsh. Chem.* **2009**, *140*, 901−907.

(15) Bognanno, M.; La Fauci, L.; Ritieni, A.; Tafuri, A.; De Lorenzo, A.; Micari, P.; Di Renzo, L.; Ciappellano, S.; Sarullo, V.; Galvano, F. Survey of the Occurrence of Aflatoxin M1 in Ovine Milk by HPLC and its Confirmation by MS. *Mol. Nutr. Food Res.* **2006**, *50*, 300−305.

(16) Santini, A.; Ferracane, R.; Meca, G.; Ritieni, A. Comparison and Improvement of the Existing Methods for the Determination of Aflatoxins in Human Serum by LC−MS/MS. *Anal. Methods* **2010**, *2*, 884.

(17) Hussain, I.; Anwar, J.; Asi, M. R.; Munawar, M. A.; Kashif, M. Aflatoxin M1 Contamination in Milk from Five Dairy Species in Pakistan. *Food Control* **2010**, *21*, 122−124.

(18) Zheng, M. Z.; Richard, J. L.; Binder, J. a Review of Rapid Methods for the Analysis of Mycotoxins. *Mycopathologia* **2006**, *161*, 261−273.

(19) Pei, S. C.; Zhang, Y. Y.; Eremin, S. A.; Lee, W. J. Detection of Aflatoxin M1 in Milk Products from China by ELISA Using Monoclonal Antibodies. *Food Control* **2009**, *20*, 1080−1085.

(20) Jans, H.; Liu, X.; Austin, L.; Maes, G.; Huo, Q. Dynamic Light Scattering As a Powerful Tool for Gold Nanoparticle Bioconjugation and Biomolecular Binding Studies. *Anal. Chem.* **2009**, *81*, 9425−9432.

(21) Dai, Q.; Liu, X.; Coutts, J.; Austin, L.; Huo, Q. A One-Step Highly Sensitive Method for DNA Detection Using Dynamic Light Scattering. *J. Am. Chem. Soc.* **2008**, *130*, 8138−8139.

(22) Liu, X.; Dai, Q.; Austin, L.; Coutts, J.; Knowles, G.; Zou, J.; Chen, H.; Huo, Q. A One-Step Homogeneous Immunoassay for Cancer Biomarker Detection Using Gold Nanoparticle Probes Coupled with Dynamic Light Scattering. *J. Am. Chem. Soc.* **2008**, *130*, 2780−2782.

(23) Shang, L.; Wang, Y.; Jiang, J.; Dong, S. pH-Dependent Protein Conformational Changes in Albumin: Gold Nanoparticle Bioconjugates: A Spectroscopic Study. *Langmuir* **2007**, *23*, 2714−2721.

(24) Radoi, A.; Targa, M.; Prieto-Simon, B.; Marty, J. L. Enzyme-Linked Immunosorbent Assay (ELISA) Based on Superparamagnetic Nanoparticles for Aflatoxin M1 Detection. *Talanta* **2008**, *77*, 138−43.

(25) Frens, G. Controlled Nucleation for the Regulation of the Particle Size in Monodisperse Gold Suspensions. *Nature* **1973**, *241*, 20−22.

(26) Brewer, S. H.; Glomm, W. R.; Johnson, M. C.; Magne, K.; Franzen, S. Probing BSA Binding to Citrate-Coated Gold Nanoparticles and Surfaces. *Langmuir* **2005**, *21*, 9303−9307.

(27) Khlebtsov, B. N.; Khlebtsov, N. G. On the Measurement of Gold Nanoparticle Sizes by the Dynamic Light Scattering Method. *Colloid J.* **2011**, *73*, 118−127.

(28) Bjorck, L.; Kronvall, G. Purification and Some Properties of Streptococcal Protein G, a Novel IgG-Binding Reagent. *J. Immunol.* **1984**, *133*, 969−974.